Journal of Electrical Engineering and Computer (JEECOM)
Vol. 8, No. 2 (2026), DOI: 10.33650/jeecom.v8i2.17057
p-ISSN: 2715-0410; e-ISSN: 2715-6427

Neuro-Fuzzy Green-Time Allocation for Oversaturated Four-Way Signalized Intersections

Ifan Wiranto [1], Yuliyanti Kadir [2]
[1] Department of Electrical Engineering, Universitas Negeri Gorontalo, Gorontalo, Indonesia
[2] Department of Civil Engineering, Universitas Negeri Gorontalo, Gorontalo, Indonesia

Article Info

Article history:

Received August 21, 2026
Revised September 03, 2026
Accepted September 04, 2026

Keywords:

Adaptive traffic light
ANFIS
Green-time allocation
Oversaturated intersection
Queue control

ABSTRACT

Fixed-time traffic signals allocate a constant green duration regardless of how vehicle demand fluctuates across approaches. That rigidity becomes critical once an approach enters oversaturation, that is, once its degree of saturation x, the ratio of the arrival rate per cycle to the capacity the signal makes available per cycle, reaches or exceeds unity, so that a residual queue is carried over from one cycle to the next and successive residuals accumulate. This study designs and simulates an adaptive green-time allocation controller based on an Adaptive Neuro-Fuzzy Inference System (ANFIS) with two inputs, aggregate phase queue length (Q) and maximum approach waiting time (W), for a four-way intersection operated from undersaturated to oversaturated conditions. The training data are not arbitrary: they are generated from a queue-actuated green-time formula whose three terms, queue discharge time, startup lost time and an anti-starvation priority proportional to normalized waiting time, are individually grounded in signal-timing theory, and whose parameters are reported in full. The model, using three Gaussian membership functions per input, nine first-order Sugeno rules and hybrid learning, was trained and validated on an 80:20 split of 180 data pairs and reached a testing RMSE of 2.39 s and an MAE of 1.87 s, that is, 2.1% of the 115-second output range. Performance was then evaluated over a 100-cycle discrete-event simulation with Poisson arrivals against fixed-time control at a constant 30 s green, using an identical queue-update mechanism. Under the baseline plan the effective capacity is 7 vehicles per approach per cycle, and the three scenarios in which at least one approach exceeds it (x = 1.14) are exactly the scenarios in which the fixed-time queue grows linearly with a strictly positive drift and in which the proposed controller yields improvements of 68.6% to 87.1%. In the four scenarios in which no approach exceeds capacity the improvement is 0.8% to 10.0%. The benefit of neuro-fuzzy green-time allocation is therefore concentrated in, and structurally explained by, the oversaturated regime.

Corresponding Author:
Ifan Wiranto,
Department of Electrical Engineering, Universitas Negeri Gorontalo, Gorontalo 96554, Indonesia
Email: ifan_te@ung.ac.id ; Orchid ID : 0000-0002-1117-6613

INTRODUCTION

The rapid growth in the number of vehicles in urban areas places substantial pressure on existing road infrastructure, and the deficit becomes visible first at signalized intersections, where capacity is rationed in time rather than in space. Conventional fixed-time traffic light systems allocate the same green duration to every approach in every cycle, without reference to the vehicle volume actually present [1]. The consequence of that rigidity is not uniform; it depends on the operating regime of the approach. So long as an approach is undersaturated, that is, so long as its degree of saturation $x = \lambda/c$, the ratio of the arrival rate λ per cycle to the capacity c that the signal makes available to that approach per cycle, remains below unity, the queue formed during red is fully discharged during the following green and the queue length fluctuates about a finite mean. Once x reaches or exceeds unity the approach becomes oversaturated: the green interval is no longer long enough to clear the accumulated queue, a residual queue is carried over into the next cycle, and successive residuals compound, so that the expected queue grows at a rate of (λ - c) vehicles per cycle and admits no steady state for as long as the demand persists [2]. Oversaturation is therefore a qualitatively different regime rather than a more severe degree of congestion: delay formulations calibrated for undersaturated operation lose their validity there, and the residual queue, not the average delay, becomes the quantity that discriminates between control strategies [2], [3]. This study is concerned with green-time allocation precisely in that regime, where fixed-time control fails structurally rather than merely inefficiently.

Adaptive Traffic Signal Control (ATSC) was developed to remove this rigidity by adjusting signal duration to prevailing conditions, and the field has been mapped in recent comprehensive reviews [4], [1]. Four families of methods dominate the current literature. Rule-based fuzzy controllers translate the engineer's linguistic judgement about queues and waiting times directly into a rule base [5], [6], [7], [8], [9]. Learning-based predictors estimate the short-term traffic state with neural architectures and drive the signal from that prediction [10], [11]. Reinforcement learning and deep reinforcement learning acquire a control policy from interaction with a simulated environment [12], [13], [14]. Metaheuristic search optimizes a timing plan against an explicit objective function [15], [16]. The Adaptive Neuro-Fuzzy Inference System (ANFIS) sits deliberately between the first and the third of these families: it retains the interpretable rule structure of a first-order Sugeno fuzzy system while obtaining its membership-function and consequent parameters from data through a hybrid least-squares and gradient-descent scheme [17], and it has been applied to signal control in a range of settings [18], [19], [20], [21].

Read across these families rather than in sequence, the reported work shares one structural weakness rather than a set of separate ones: in each case the supervisory signal is asserted rather than derived. In the fuzzy family the rule table is itself the supervisory signal, and it is written by hand [5], [7], [8]. In the reinforcement-learning family the reward function plays that role, and it is engineered, with the sensitivity of the resulting policy to that engineering a recurring caveat [12], [14]. In the ANFIS family the training table plays that role, and it is typically presented without derivation or generated from a hand-written fuzzy rule base, so that the network reproduces the designer's intuition at one further remove [18], [19], [20], [21]. The consequence is common to all three: when such a controller performs well, the result cannot be attributed to a defensible control principle rather than to a fortunate choice of supervision. Ali et al. [22] are the closest exception, coupling fuzzy inference to the Webster and modified-Webster timing formulas and thereby anchoring at least the cycle-length decision in signal-timing theory; the present study extends that principle from the cycle to the per-phase green allocation, and from the inference stage to the training stage. A second observation follows from reading the same literature against the regime distinction drawn above. The reported evaluations are overwhelmingly situated in the undersaturated or near-saturated range, and improvement is reported as a single aggregate figure. Where fixed-time control is not merely inefficient but unstable, and where an adaptive controller therefore has the most to offer, the evidence base is comparatively thin.

This study designs and simulates an ANFIS-based green-time allocation controller for a four-way intersection, and makes three contributions stated relative to the ANFIS-based signal controllers reviewed above. First, the supervision is traceable. Every training triple (Q, W, T) is produced by an explicit queue-actuated green-time formula whose three terms, queue discharge time, startup lost time and an anti-starvation priority proportional to normalized waiting time, are individually interpretable in signal-timing terms [23], [24], and whose parameters are reported in full, so that the mapping the network learns can be audited term by term rather than accepted on trust. Second, the supervisor and the evaluator are closed on each other. The saturation service rate that appears in the training formula is the same rate that governs vehicle discharge in the evaluation simulation, and the queue-update mechanism is identical for the proposed controller and for the fixed-time baseline, so that any difference in outcome is attributable to the green-duration decision alone and not to a mismatch between a training model and a separate evaluation model, such as arises when a controller is trained on a queueing abstraction and evaluated in a microsimulator. Third, the evaluation is organized around the saturation regime. Seven arrival scenarios spanning per-approach degrees of saturation from x = 0.29 to x = 1.14 are simulated, each scenario is classified by the number of approaches it drives beyond capacity, and improvement is reported against that classification, so that the result identifies where the benefit of adaptive green-time allocation becomes decisive rather than marginal.

LITERATURE REVIEW

2.1. Neuro-Fuzzy Inference and What the Argument Requires from It

The controller used here is a first-order Sugeno fuzzy inference system whose parameters are learned rather than designed, and only those properties on which the argument of this paper actually depends are recalled. A Sugeno rule takes the form IF Q is A_i AND W is B_j THEN $f_{ij} = p_{ij}Q + q_{ij}W + r_{ij}$: its consequent is a linear function of the inputs rather than a fuzzy set. Two consequences matter here. The aggregated output is a firing-strength-weighted average of linear functions and is therefore continuous and differentiable in the inputs, which is what permits a green-time surface to be interpolated smoothly between rules instead of switching discretely between them; and the consequent parameters enter that output linearly, which is what permits them to be estimated in closed form. ANFIS exploits the second property directly. It realizes the Sugeno system as a five-layer adaptive network whose layers perform fuzzification, rule firing, normalization, rule-consequent evaluation and aggregation, and trains it under a hybrid scheme in which the linear consequent parameters are estimated by least squares in the forward pass while the premise parameters, the centres and widths of the membership functions, are updated by gradient descent in the backward pass [17]. The property that matters for what follows is a negative one: the shape of the learned control surface is not asserted by the designer but inherited from the data on which the network is trained. The provenance of that data is therefore the substantive design decision, and it is the decision this study makes explicit.

2.2. Green-Time Allocation at Signalized Intersections

Green-time allocation is the problem of distributing a finite cycle among approaches that compete for it, and any allocation rule, however it is implemented, must supply three ingredients: a measure of demand, a model of how that demand discharges once green begins, and bounds within which the resulting duration must fall. Fixed-time control fixes all three offline. The classical Webster procedure and its modern refinements determine cycle length and splits from historical flow ratios so as to minimize expected delay, and they remain the reference against which actuated and adaptive plans are assessed [23]. Their discharge model rests on the saturation flow rate, the rate at which a standing queue leaves the stop line under sustained green, and on the startup lost time incurred while the first vehicles react and accelerate; recent empirical work at fully actuated intersections shows that it is the fraction of the available green actually used at saturation flow, rather than the nominal green itself, that governs realized capacity [24]. The bounds are supplied by a minimum green, dictated by safety and pedestrian clearance, and a maximum green, which prevents an approach with persistent demand from starving the competing movements.

Adaptive strategies retain these three ingredients but resolve them online. Demand is measured from detectors or, increasingly, estimated in real time from partial detection [3] or predicted from recent history with machine-learning models [10], [11]. The discharge model is either retained analytically, as when fuzzy inference is coupled to the Webster formula [22], or absorbed implicitly into a learned policy [12], [13]. The bounds survive in every case, because minimum and maximum green are safety and fairness constraints rather than modelling choices. Metaheuristic formulations optimize the allocation against an explicit delay objective and demonstrate the gain available from departing from a fixed split [16], while connected-vehicle formulations extend the same allocation problem to coordinated corridors [1]. The controller proposed in this study operates on the same three ingredients: it takes its demand measure from queue length and waiting time, its discharge model from an explicit saturation service rate, and its bounds from stated minimum and maximum green values, and then learns the resulting mapping rather than evaluating it analytically at every cycle.

2.3. Oversaturated Operation and Its Consequences for Control

The distinction between undersaturated and oversaturated operation is one of kind, not of degree. Let c denote the number of vehicles an approach can discharge in one cycle under a given timing plan, and λ the number that arrive in that cycle. When $\lambda < c$ the queue process is stable: the residual at the end of each cycle returns to zero, queue length fluctuates about a finite mean determined by the variability of arrivals, and delay is well approximated by the standard undersaturated formulations. When $\lambda \geq c$ the queue process is transient: a residual of $(\lambda - c)$ vehicles survives every cycle, residuals accumulate, and the expected queue after k cycles is $Q(0) + (\lambda - c)k$, which increases without bound as k grows for as long as the demand persists. Empirical work on oversaturation accordingly treats it as a distinguishable regime with its own loading, operation and recovery phases, and characterizes it through spatial and temporal oversaturation indices derived from trajectory data rather than through average delay [2].

Two implications for controller evaluation follow, and both are adopted in this study. First, the performance measure must remain well defined in both regimes. Average delay does not: formulations calibrated for undersaturated operation diverge from observed values once the degree of saturation approaches unity, whereas the residual queue remains finite over any finite horizon, is directly observable, and orders the two regimes consistently [2], [3]. Second, the objective itself changes. Below saturation the controller is minimizing an already-bounded delay; at and above saturation it is competing against divergence, and the relevant question is whether it can hold the queue stable at all, not by how many seconds it improves an average. An evaluation that reports a single improvement figure aggregated across regimes therefore conceals the result of interest, which is where the transition between the two situations occurs.

2.4. ANFIS in Signal Control and the Residual Gap

Within this landscape ANFIS occupies a specific position. Jutury et al. [18] developed an adaptive neuro-fuzzy multi-mode controller that switches between operating modes according to live traffic and heterogeneous vehicle composition, evaluated on a city-scale SUMO network, and reported improvement over both fixed-time and single-mode adaptive baselines. Vuong et al. [19] tested an ANFIS controller under the mixed-traffic conditions of Hanoi in a coupled VISSIM-MATLAB environment, and Zeynal et al. [20] addressed the input-selection problem, showing that which variables are presented to the network materially affects control accuracy. Olayode et al. [21] compared a plain ANFIS model with a genetic-algorithm-tuned variant for vehicular flow at intersections and reported an improved fit for the tuned model, confirming that the neuro-fuzzy family remains competitive for traffic-state modelling. Ali et al. [22] took the complementary route of combining fuzzy inference with the Webster and modified-Webster formulas, which is the closest published precedent for the principle adopted here, namely that a classical timing formula and a computational-intelligence method are complementary rather than alternative.

The review by Agrahari et al. [4] classifies ATSC studies by number of intersections and by technique, and observes that fixed-time systems still dominate as the simulation baseline. Two gaps remain after this reading. The first concerns provenance: across [18], [19], [20] and [21] the training data are either drawn from simulator runs under an unstated control policy or generated from a hand-written fuzzy rule base, so that the input-output mapping the network acquires cannot be traced to a stated traffic-engineering principle, and a reported gain cannot be separated from the choice of supervision. The second concerns regime: the scenarios reported are predominantly undersaturated or near-saturated, and where heavy demand is examined the degree of saturation is not stated, so the reader cannot determine whether the baseline was merely inefficient or actually unstable. This study addresses the first gap by deriving the training data from a queue-actuated formula stated in full, and the second by classifying every evaluated scenario by its per-approach degree of saturation before reporting improvement.

METHOD

3.1. System Design

The system controls an isolated four-way intersection with approaches North, South, East and West, operated in two signal phases: Phase 1 serves North and South, Phase 2 serves East and West. Turning movements and pedestrian phases are not modelled separately, and the intersection is treated as isolated, that is, without coordination with adjacent signals. In each phase the controller receives two aggregate input variables, the combined queue length across the two approaches served by that phase, $Q_p = Q_i + Q_j$, and the maximum waiting time among those approaches, $W_p = \max(W_i, W_j)$, and returns the green duration T_p for that phase. Aggregating at phase level rather than approach level is deliberate, because green time is a phase-level decision variable: both approaches in a phase receive the same green, so the controller must reason about their joint demand. The maximum rather than the mean waiting time is used so that a single long-waiting approach cannot be masked by a recently served one.

3.2. Queue-Actuated Green-Time Formula and Its Parameters

The training data are generated from the queue-actuated green-time formula in (1), stated here at phase level with phase index p.

$$T_p(Q_p, W_p) = clip(Q_p/s + t_0 + k_u \cdot (W_p/W_{max}) \cdot (T_{max} - T_{min}), T_{min}, T_{max}) \quad (1)$$

The formula is the sum of three terms, each with a distinct role and each grounded in a distinct element of signal-timing practice, followed by a saturation to the admissible range. The first term, Q_p/s, is the queue discharge time: the time required for a standing queue of Q_p vehicles to cross the stop line at the saturation service rate s. It is the demand-responsive core of the formula and corresponds to the discharge component of classical timing procedures [23]. The second term, t_0, is the startup lost time, the interval at the beginning of green during which the first vehicles react and accelerate and flow has not yet reached saturation; adding it compensates for the fact that the nominal green exceeds the green actually used at saturation flow [24]. The third term, $k_u(W_p/W_{max})(T_{max} - T_{min})$, is an anti-starvation priority: it converts the normalized waiting time W_p/W_{max}, which lies in [0, 1], into an additive green increment scaled to the admissible range, so that a phase which has waited long receives additional green even when its instantaneous queue is short. Without this term a phase with persistently low queue could be indefinitely deferred by the competing phase under asymmetric demand. The outer clip enforces the operational bounds T_{min} and T_{max}.

All parameter values, their units, their role in (1) and the basis on which each value was set are given in Table 1. Two of the bounds deserve comment because they are operational rather than modelling choices. The maximum green T_{max} = 120 s bounds the delay that a saturated phase can impose on the competing phase and caps the cycle length; it is the parameter that determines the highest capacity the proposed controller can deliver, and it is therefore the binding constraint in the oversaturated scenarios of Section 4. The minimum green T_{min} = 5 s is the value used to generate the training data and to bound the controller output in the simulation; it is shorter than the minimum green that pedestrian clearance would require at a field installation, and in a field deployment it would be raised to the value dictated by the crossing width and the applicable design standard. Because every scenario examined here is demand-limited rather than minimum-green-limited, this bound is not active in any of the reported results.

Table 1. Parameters of the queue-actuated green-time formula in (1)

Symbol	Value	Unit	Role in (1)	Basis for the value
s	0.5	veh/s	Saturation service rate governing queue discharge	1800 veh/h, the conventional order of magnitude of saturation flow per lane; set equal to the discharge rate used in the simulation so that (1) and (2) are consistent
t_0	3	s	Startup lost time added to every green interval	Within the 2-4 s range conventionally assumed for reaction and acceleration of the first vehicles in a standing queue
k_u	0.5	-	Weight of the anti-starvation priority term	Set so that a phase at maximum normalized waiting time gains at most half of the admissible green range
W_{max}	180	s	Normalizing constant that maps waiting time onto [0, 1]	Upper limit of the waiting-time range of the training grid (Section 3.3)
T_{min}	5	s	Lower bound of the green duration	Minimum green; not binding in any reported scenario
T_{max}	120	s	Upper bound of the green duration	Maximum green; bounds cycle length and the delay imposed on the competing phase

3.3. Generation of the Training Set

Equation (1) is evaluated on a regular grid over the two input variables to produce the training set. Queue length Q_p is sampled over the range of 5 100 and waiting time W_p over the range of 10 to 170, giving 180 input-output triples in total. The grid is chosen to span the range of queue and waiting-time values that the intersection actually reaches in the simulation scenarios of Section 3.5, including the oversaturated ones, so that the network is not required to extrapolate beyond its training domain during evaluation. Because (1) is deterministic, the resulting mapping carries no observation noise; the generalization error reported in Section 4.1 therefore measures the ability of the network to reproduce a known function rather than to filter noise.

3.4. ANFIS Architecture and Training

The ANFIS model is designed with two input variables (Q, W), each represented by three Gaussian membership functions, producing nine first-order Sugeno rules (3 × 3), as shown in Figure 1.

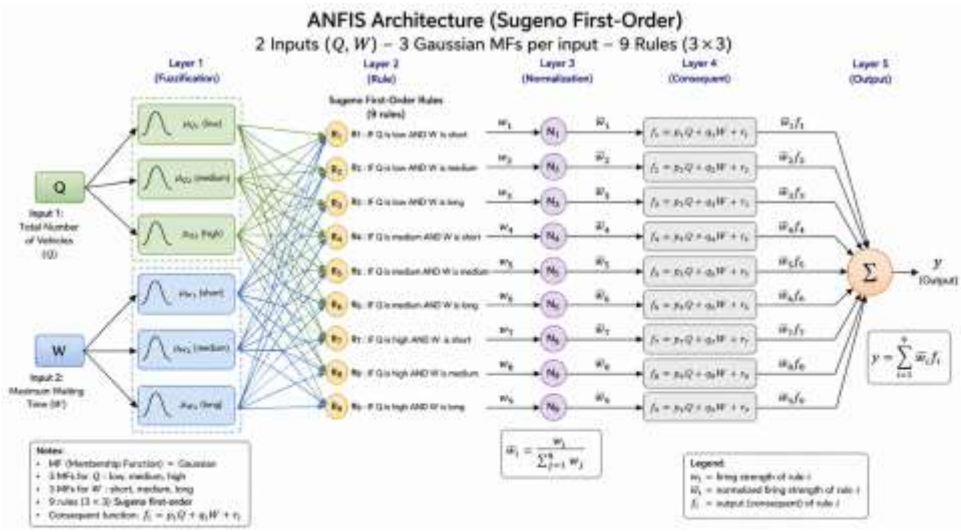

Figure 1. Five-layer ANFIS architecture with two inputs (Q, W) and nine first-order Sugeno rules

Each rule i has a linear consequent of the form $f_i = p_iQ + q_iW + r_i$, and the final output is computed as the weighted average of the firing strengths of all rules, following the five-layer ANFIS architecture [17]. Training uses a hybrid learning scheme: the consequent parameters p_i, q_i, and r_i are estimated using Least-Squares Estimation at each epoch, while the premise parameters (the center and width of the Gaussian functions) are updated via gradient descent based on the prediction error. The data are randomly split into 80% training data (144 pairs) and 20% testing data (36 pairs) to evaluate the generalization ability of the model.

3.5. Simulation Scheme, Fixed-Time Baseline and Consistency Between the Models

System performance is evaluated through a discrete-event simulation of 100 signal cycles at the same four-way intersection. The initial queues are $Q_N = 7$, $Q_S = 6$, $Q_E = 8$ and $Q_W = 10$ vehicles and the initial waiting time is 30 s on every approach. Arrivals at approach j during a cycle are drawn independently from a Poisson distribution with mean λ_j vehicles per cycle. Both symmetric scenarios, in which λ is equal on all approaches, and asymmetric scenarios, in which it differs, are simulated. The number of vehicles served at approach j during cycle k is given by (2) and the queue is updated by (3), where $A_j(k)$ is the Poisson arrival count in that cycle.

$$served_j(k) = \min(Q_j(k), s \cdot T_p(k)/2) \quad (2)$$

$$Q_j(k+1) = Q_j(k) - served_j(k) + A_j(k), \quad A_j(k) \sim Poisson(\lambda_j) \quad (3)$$

Equations (1) and (2) are stated at different levels of aggregation, and the relation between them is the following. Equation (1) is a phase-level statement: it returns the green duration required to discharge the combined queue Q_p of the two approaches served by phase p, so the discharge capacity it implies for the phase as a whole is $s \cdot T_p$. Equation (2) is an approach-level statement: the two approaches served by that phase draw on the same phase capacity, so each receives $s \cdot T_p/2$, and their total is $2 \cdot s \cdot T_p/2 = s \cdot T_p$, which is exactly the phase capacity implied by the Q_p/s term in (1). The factor of one half in (2) is therefore not an independent modelling assumption but the per-approach share of the phase capacity that (1) allocates, and the two equations are consistent at the level at which each is defined. One residual discrepancy remains and is stated for completeness: (1) adds the startup lost time t_0 to the green, whereas (2) applies the full duration T_p at the saturation rate, so the model grants $s \cdot t_0 = 1.5$ vehicles per phase per cycle more capacity than the discharge term alone requires. This margin is conservative in the direction of clearing the queue, is identical in the proposed and the baseline scenarios, and therefore does not bias the comparison between them.

Equations (2) and (3) are applied identically in both scenarios. The sole difference is the origin of T_p: for the proposed controller it is the ANFIS prediction, and for the fixed-time baseline it is a constant 30 s in both phases. Holding the queue-update mechanism identical is what allows the difference in results to be attributed to the green-duration decision alone rather than to a difference in the underlying simulation model. The evaluation metric is the average total queue across the four approaches per cycle. This metric is preferred over average delay because delay formulations calibrated for undersaturated operation lose validity once the degree of saturation approaches or exceeds unity, whereas the residual queue remains well defined and directly observable in both regimes [2], [3].

3.6. Capacity and Degree of Saturation of the Evaluated Scenarios

Because the classification of scenarios into regimes governs the interpretation of the results, the capacity implied by the baseline timing plan is stated explicitly. Under the fixed-time baseline T = 30 s, so by (2) the capacity available to each approach in one cycle is given by (4), and because vehicles are discharged as whole units the effective integer capacity is c_{eff} = 7 vehicles per approach per cycle. The degree of saturation of approach j and its per-cycle queue drift then follow from (5) and (6).

$$c = s \cdot T/2 = 0.5 \cdot 30/2 = 7.5 \text{ vehicles per cycle} \quad (4)$$

$$x_j = \lambda_j / c_{eff} \quad (5)$$

$$\delta_j = \max(\lambda_j - c_{eff},\ 0) \quad (6)$$

An approach with $x_j < 1$ has $\delta_j = 0$ and a stable queue; an approach with $x_j \geq 1$ has $\delta_j > 0$ and a queue that grows linearly in the number of cycles. The corresponding quantities for the proposed controller are bounded by its maximum green: at T_{max} = 120 s the per-approach capacity reaches $s \cdot T_{max}/2$ = 30 vehicles per cycle, so the highest arrival rate examined here, $\lambda = 8$, corresponds to $x = 0.27$ under the proposed controller, and the queue remains in the stable regime by construction.

RESULTS AND DISCUSSION

4.1. Training and Model Validation Results

The ANFIS training process showed stable convergence, with the training error decreasing sharply over the first 150 epochs and settling at a low value after approximately 200-250 epochs out of a total of 500 training epochs (Figure 2), indicating that the hybrid learning scheme successfully adjusted the premise and consequent parameters without significant signs of overfitting.

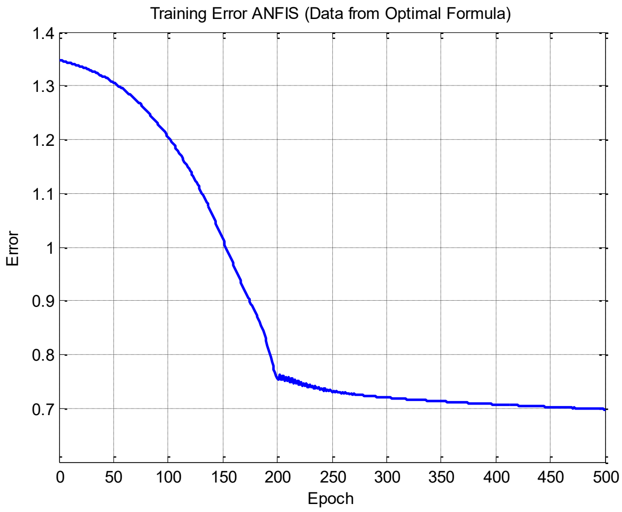

Figure 2. ANFIS training error convergence curve versus number of epochs

The control surface learned by ANFIS (Figure 3) shows a pattern consistent with the queue-actuated control formula in (1): green duration increases monotonically with both queue length (Q) and waiting time (W), with a saturation effect at T_{max} = 120 seconds when both input variables are high. This smooth, monotonic surface pattern indicates that ANFIS successfully learned the underlying functional structure of the training data, rather than merely performing unstable local interpolation.

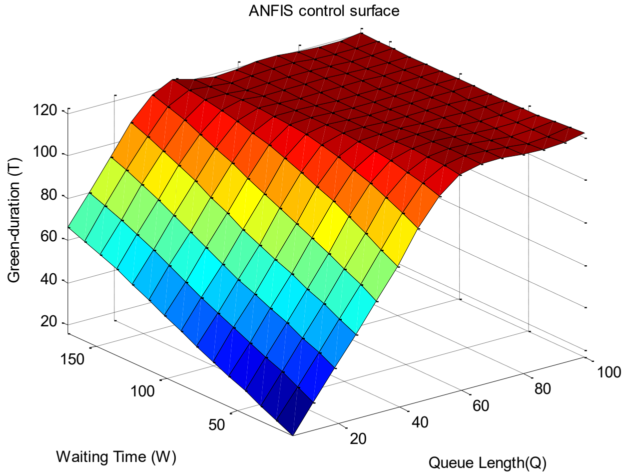

Figure 3. ANFIS control surface with respect to variables Q and W

On the testing data (36 pairs not seen during training), the model achieved an RMSE of 2.39 seconds and an MAE of 1.87 seconds against a target green-duration range of 5-120 seconds, indicating good generalization performance (Figure 4). Given an output range of 115 seconds, an RMSE of 2.39 seconds corresponds to a relative error of less than 2.1%, an accuracy level that is adequate for traffic-signal control applications operating on a second-by-second timescale. This result indicates that training data derived from a deterministic formula produce a consistent input-output mapping that is readily learned by the ANFIS model.

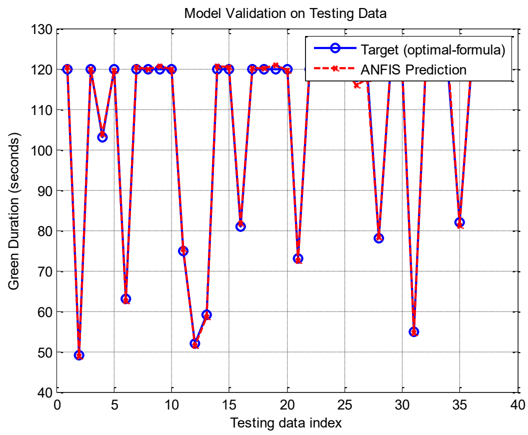

Figure 4. Comparison of target (optimal-formula) green duration and ANFIS prediction on the testing data

4.2. Saturation Classification of the Evaluated Scenarios

Before the two controllers are compared, the seven arrival scenarios are classified by the regime into which they drive the fixed-time baseline, using (5) and (6) with $c_{eff} = 7$ vehicles per approach per cycle. Table 2 reports the resulting degrees of saturation, the number of oversaturated approaches and the aggregate queue drift of each scenario. Three scenarios drive at least one approach beyond capacity and four do not, and this partition, rather than total arrival volume, is what organizes the results that follow.

Table 2. Degree of saturation and queue drift of the seven arrival scenarios under the fixed-time baseline ($c_{eff} = 7$ veh/approach/cycle)

Arrival rate λ (N/S/E/W)	**Degree of saturation x (N/S/E/W)**	**Oversaturated approaches**	**Aggregate drift (veh/cycle)**	**Regime**
3 / 3 / 3 / 3	0.43 / 0.43 / 0.43 / 0.43	0	0	Undersaturated, symmetric
5 / 5 / 5 / 5	0.71 / 0.71 / 0.71 / 0.71	0	0	Undersaturated, symmetric

Arrival rate λ (N/S/E/W)	Degree of saturation x (N/S/E/W)	Oversaturated approaches	Aggregate drift (veh/cycle)	Regime
8 / 8 / 8 / 8	1.14 / 1.14 / 1.14 / 1.14	4	4	Fully oversaturated
5 / 5 / 2 / 2	0.71 / 0.71 / 0.29 / 0.29	0	0	Undersaturated, asymmetric
8 / 8 / 5 / 5	1.14 / 1.14 / 0.71 / 0.71	2	2	Partially oversaturated
8 / 5 / 8 / 5	1.14 / 0.71 / 1.14 / 0.71	2	2	Partially oversaturated
8 / 3 / 5 / 2	1.14 / 0.43 / 0.71 / 0.29	1	1	Partially oversaturated

4.3. Comparative Simulation Results

Table 3 summarizes the 100-cycle simulation results for the same seven scenarios, reporting the average total queue under each controller and the resulting improvement.

Table 3. Summary of 100-cycle simulation results: proposed ANFIS controller versus fixed-time control

Vehicle Arrival Rate λ (North/South/East/West)	Average Total Queue – ANFIS	Average Total Queue – Fixed-Time	Improvement (%)
3 / 3 / 3 / 3	12.06	12.16	0.8
5 / 5 / 5 / 5	20.52	22.80	10.0
8 / 8 / 8 / 8	32.12	248.58	87.1
5 / 5 / 2 / 2	14.29	15.41	7.3
8 / 8 / 5 / 5	26.08	138.82	81.2
8 / 5 / 8 / 5	26.19	137.81	80.5
8 / 3 / 5 / 2	17.78	56.59	68.6

The seven scenarios separate cleanly along the classification of Table 2, and the separation is sharper than any separation by total demand. In the four scenarios in which no approach is oversaturated the improvement lies between 0.8% and 10.0%; in the three scenarios in which at least one approach is oversaturated it lies between 68.6% and 87.1%. There is no intermediate case. Total arrival volume does not produce this separation on its own: scenario (5, 5, 5, 5), with a total of 20 vehicles per cycle, yields a 10.0% improvement, while scenario (8, 3, 5, 2), with a total of 18 vehicles per cycle, yields 68.6%. What distinguishes them is not how many vehicles arrive at the intersection but whether any single approach receives more than the seven vehicles per cycle that a fixed 30-second green can discharge. In the undersaturated scenarios the fixed green is already sufficient to clear each queue within the cycle, so adaptive allocation can only trim the residual fluctuation, and the improvement grows from 0.8% at $x = 0.43$ to 10.0% at $x = 0.71$ as the margin between arrival and capacity narrows.

Within the oversaturated group, the behaviour of the fixed-time baseline is ordered by the aggregate drift rather than by total demand. The mean total queue under fixed-time control is 56.59 vehicles at a drift of 1 vehicle per cycle, 137.81 and 138.82 vehicles at a drift of 2, and 248.58 vehicles at a drift of 4, which is the ordering predicted by (5) and (6): with drift δ the queue after k cycles is the surviving initial residual plus δk, so its mean over a 100-cycle horizon rises approximately in proportion to δ. That the three asymmetric oversaturated scenarios (8, 8, 5, 5) and (8, 5, 8, 5) yield almost identical outcomes, 81.2% and 80.5%, despite distributing the same excess demand across phases in different ways, is consistent with the same account: what governs the outcome is how much demand exceeds capacity in total, not which approaches carry it. The proposed controller, whose per-approach capacity extends to 30 vehicles per cycle at maximum green, keeps every scenario in the stable regime, and its mean total queue rises only from 12.06 to 32.12 vehicles across the entire range of demand examined. Figures 5 and 6 contrast the two regimes directly: the light symmetric scenario produces a bounded, stationary queue trajectory under both controllers, whereas the heavy symmetric scenario separates them into a bounded trajectory and a linearly growing one.

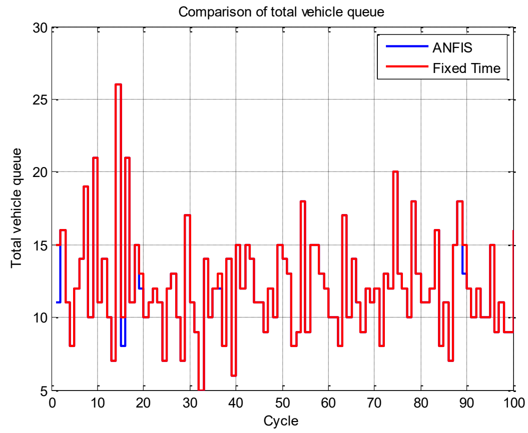

Figure 5. Comparison of total vehicle queue per cycle under light, symmetric traffic conditions (λ = 3 for all approaches)

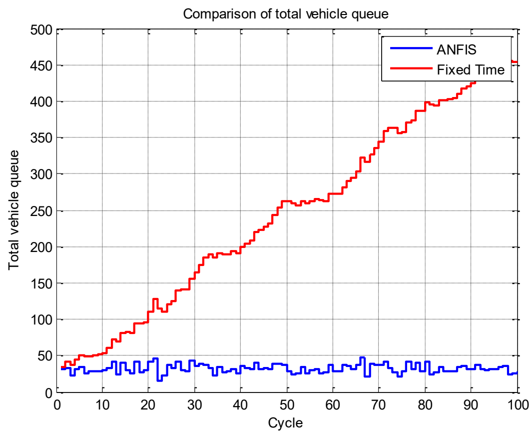

Figure 6. Comparison of total vehicle queue per cycle under heavy, symmetric traffic conditions (λ = 8 for all approaches), showing the linear, divergent queue growth of fixed-time control when λ exceeds the per-approach capacity

4.4. The Nature of the Divergence Under Fixed-Time Control

The term used to describe the fixed-time trajectory in the heaviest scenario requires precision. Under fixed-time control at λ = 8 on every approach, each approach receives an effective capacity of 7 vehicles per cycle and therefore retains a residual of 1 vehicle per cycle, giving an aggregate drift of 4 vehicles per cycle across the intersection. The expected total queue after k cycles is Q(0) + 4k, a linear function of k with strictly positive slope that admits no finite limit as k tends to infinity. The growth is therefore unbounded as a property of the model, not merely as a description of the simulated trace: it follows from λ > c and is not an artefact of the 100-cycle horizon, and extending the horizon would extend the growth rather than reveal a plateau. What Figure 6 shows is the finite-horizon manifestation of that property, an approximately linear increase from about 30 vehicles in the opening cycles to more than 400 by cycle 100, at a rate consistent with the predicted slope. The qualification that does apply is the converse one: the divergence holds only for as long as the arrival rate is sustained above capacity, and a real demand profile that falls back below capacity would enter the recovery phase and discharge the accumulated residual [2]. Within the constant-λ regime examined here, however, the fixed-time baseline has no stable operating point, and this is the structural reason why the improvement in the oversaturated scenarios is an order of magnitude larger than in the undersaturated ones: the comparison is no longer between two bounded queues of different size, but between a bounded queue and a divergent one. In contrast, the proposed controller extends the green of the loaded phase toward the T_{max} = 120-second bound, which raises the per-approach capacity to 30 vehicles per cycle, restores λ < c, and holds the total queue within the range of 25 to 40 vehicles for the whole simulation.

Taken together, these results are consistent with the hypothesis that motivated the design. Because the training data are derived directly from a queue-actuated formula that accounts for discharge time, startup lost time and anti-starvation priority, the learned model reproduces a green-allocation strategy that is close to the one the formula prescribes, and the advantage of that strategy is largest precisely where the fixed alternative is not merely suboptimal but unstable. The corollary is equally important for practice: in the undersaturated regime, which covers four of the seven scenarios examined, the measured benefit of adaptive allocation is between 0.8% and 10.0%, which may not justify the additional detection and control infrastructure. The case for neuro-fuzzy green-time allocation rests on the oversaturated regime.

CONCLUSION

This study designed and simulated an ANFIS-based green-time allocation controller for a four-way signalized intersection in which the training data are derived explicitly and traceably from a queue-actuated formula whose three terms, queue discharge time, startup lost time and an anti-starvation priority, are each grounded in signal-timing theory and whose parameters are reported in full, rather than from a data table of unstated origin as is common in prior ANFIS studies; the trained model, with two inputs, three Gaussian membership functions per input, nine first-order Sugeno rules and hybrid learning, reached a testing RMSE of 2.39 s and an MAE of 1.87 s, that is, 2.1% of the 115-second output range, and a 100-cycle discrete-event simulation across seven Poisson arrival scenarios showed that its advantage over fixed-time control is governed by the saturation regime rather than by total demand, since in the four scenarios in which no approach exceeded the effective fixed-time capacity of seven vehicles per cycle the improvement in average total queue was between 0.8% and 10.0%, whereas in the three scenarios in which at least one approach was driven beyond that capacity, and in which the fixed-time queue therefore grew linearly with strictly positive drift and admitted no stable operating point, the improvement was between 68.6% and 87.1%, the proposed controller restoring stability by extending the green of the loaded phase toward its 120-second bound. Three limitations bound these claims and set the agenda for further work: the intersection was isolated and described by two aggregate inputs, so extension to coordinated multi-intersection control and to additional inputs such as pedestrian demand or emergency-vehicle priority remains open; arrivals were independent and Poisson, so validation against field data with correlated, platooned arrivals is required before the reported gains can be transferred to operational conditions; and the comparison was made against fixed-time control alone, so positioning the proposed controller among the alternatives, namely pure fuzzy inference [7], reinforcement and deep reinforcement learning [12], [13], metaheuristic timing optimization [16], [15], and conventional actuated control based on a Webster-type formula [23], requires a broader benchmark, ideally one in which every competing strategy is evaluated across the same range of saturation regimes rather than at a single operating point.

ACKNOWLEDGEMENTS

The authors would like to express their sincere gratitude to the Institute for Research and Community Service (LPPM), Universitas Negeri Gorontalo, for providing financial support for this research. This research was funded under Contract No. 1002/UN47.D1/PT.01.03/2026.

REFERENCES

[1] J. Li, L. Peng, K. Hou, Y. Tian, Y. Ma, S. Xu, and T. Z. Qiu, "Adaptive signal control and coordination for urban traffic control in a connected vehicle environment: A review," Digital Transportation and Safety, vol. 2, no. 2, pp. 89-111, 2023, doi: 10.48130/DTS-2023-0008.
[2] B. Huang and F. Zhang, "Analysis of traffic oversaturation based on multi-objective data," Sustainability, vol. 14, no. 15, 2022, Art. no. 9043, doi: 10.3390/su14159043.
[3] P. Pudasaini, A. Karimpour, and Y.-J. Wu, "Real-time queue length estimation for signalized intersections using single-channel advance detector data," Transportation Research Record, vol. 2677, no. 7, pp. 144-156, 2023, doi: 10.1177/03611981221151066.
[4] A. Agrahari, M. M. Dhabu, P. S. Deshpande, A. Tiwari, M. A. Baig, and A. D. Sawarkar, "Artificial intelligence-based adaptive traffic signal control system: A comprehensive review," Electronics, vol. 13, no. 19, 2024, Art. no. 3875, doi: 10.3390/electronics13193875.
[5] S. Jafari, Z. Shahbazi, and Y.-C. Byun, "Traffic control prediction design based on fuzzy logic and Lyapunov approaches to improve the performance of road intersection," Processes, vol. 9, no. 12, 2021, Art. no. 2205, doi: 10.3390/pr9122205.
[6] S. Jafari, Z. Shahbazi, and Y.-C. Byun, "Improving the road and traffic control prediction based on fuzzy logic approach in multiple intersections," Mathematics, vol. 10, no. 16, 2022, Art. no. 2832, doi: 10.3390/math10162832.
[7] V. M. Madrigal Arteaga, J. R. Perez Cruz, A. Hurtado-Beltran, and J. Trumpold, "Efficient intersection management based on an adaptive fuzzy-logic traffic signal," Applied Sciences, vol. 12, no. 12, 2022, Art. no. 6024, doi: 10.3390/app12126024.
[8] T. D. Chala and L. T. Koczy, "Intelligent fuzzy traffic signal control system for complex intersections using fuzzy rule base reduction," Symmetry, vol. 16, no. 9, 2024, Art. no. 1177, doi: 10.3390/sym16091177.
[9] F. Zahwa, C.-T. Cheng, and M. Simic, "Novel intelligent traffic light controller design," Machines, vol. 12, no. 7,

2024, Art. no. 469, doi: 10.3390/machines12070469.
[10] A. Navarro-Espinoza, O. R. Lopez-Bonilla, E. E. Garcia-Guerrero, E. Tlelo-Cuautle, D. Lopez-Mancilla, C. Hernandez-Mejia, and E. Inzunza-Gonzalez, "Traffic flow prediction for smart traffic lights using machine learning algorithms," Technologies, vol. 10, no. 1, 2022, Art. no. 5, doi: 10.3390/technologies10010005.
[11] S. A. Sayed, Y. Abdel-Hamid, and H. A. Hefny, "Artificial intelligence-based traffic flow prediction: A comprehensive review," Journal of Electrical Systems and Information Technology, vol. 10, no. 1, 2023, Art. no. 13, doi: 10.1186/s43067-023-00081-6.
[12] M. Kolat, B. Kovari, T. Becsi, and S. Aradi, "Multi-agent reinforcement learning for traffic signal control: A cooperative approach," Sustainability, vol. 15, no. 4, 2023, Art. no. 3479, doi: 10.3390/su15043479.
[13] C. Ouyang, Z. Zhan, and F. Lv, "A comparative study of traffic signal control based on reinforcement learning algorithms," World Electric Vehicle Journal, vol. 15, no. 6, 2024, Art. no. 246, doi: 10.3390/wevj15060246.
[14] A. Haydari and Y. Yilmaz, "Deep reinforcement learning for intelligent transportation systems: A survey," IEEE Trans. Intell. Transp. Syst., vol. 23, no. 1, pp. 11-32, Jan. 2022, doi: 10.1109/TITS.2020.3008612.
[15] J. Wei and Y. Ju, "Research on optimization method for traffic signal control at intersections in smart cities based on adaptive artificial fish swarm algorithm," Heliyon, vol. 10, no. 10, 2024, Art. no. e30657, doi: 10.1016/j.heliyon.2024.e30657.
[16] A. Jamal, M. T. Rahman, H. M. Al-Ahmadi, I. Ullah, and M. Zahid, "Intelligent intersection control for delay optimization: Using meta-heuristic search algorithms," Sustainability, vol. 12, no. 5, 2020, Art. no. 1896, doi: 10.3390/su12051896.
[17] A. Buriboev and A. Muminov, "Computer state evaluation using adaptive neuro-fuzzy inference systems," Sensors, vol. 22, no. 23, 2022, Art. no. 9502, doi: 10.3390/s22239502.
[18] D. Jutury, N. Kumar, A. Sachan, Y. Daultani, and N. Dhakad, "Adaptive neuro-fuzzy enabled multi-mode traffic light control system for urban transport network," Applied Intelligence, vol. 53, no. 6, pp. 7132-7153, Mar. 2023, doi: 10.1007/s10489-022-03827-3.
[19] X. C. Vuong, R.-F. Mou, T. T. Vu, and H. V. Nguyen, "An adaptive method for an isolated intersection under mixed traffic conditions in Hanoi based on ANFIS using VISSIM-MATLAB," IEEE Access, vol. 9, pp. 166328-166338, 2021, doi: 10.1109/ACCESS.2021.3135418.
[20] H. Zeynal, Z. Zakaria, A. Kor, and H. Torkamani, "An improved ANFIS based traffic flow control through a novel approach on input selection," in Proc. IEEE Int. Conf. Power Eng. Appl. (ICPEA), 2021, pp. 161-166, doi: 10.1109/ICPEA51500.2021.9417843.
[21] I. O. Olayode, L. K. Tartibu, and F. J. Alex, "Comparative study analysis of ANFIS and ANFIS-GA models on flow of vehicles at road intersections," Applied Sciences, vol. 13, no. 2, Jan. 2023, Art. no. 744, doi: 10.3390/app13020744.
[22] M. E. M. Ali, A. Durdu, S. A. Celtek, and A. Yilmaz, "An adaptive method for traffic signal control based on fuzzy logic with Webster and modified Webster formula using SUMO traffic simulator," IEEE Access, vol. 9, pp. 102985-102997, 2021, doi: 10.1109/ACCESS.2021.3094270.
[23] A. A. Rrecaj, R. Mazrekaj, and G. Hoxha, "A modified Webster model for a useful traffic signal timing plan," in Proc. Joint Int. Conf. 10th Textile Conf. and 4th Conf. Eng. Entrepreneurship (Lecture Notes on Multidisciplinary Industrial Engineering). Cham, Switzerland: Springer, 2024, pp. 108-120, doi: 10.1007/978-3-031-48933-4_11.
[24] N. C. Karabulut, M. Ozen, and O. Altintasi, "Understanding the determinants of lane inefficiency at fully actuated intersections: An empirical analysis," Sustainability, vol. 16, no. 2, 2024, Art. no. 722, doi: 10.3390/su16020722.